Redox Potential–Structure Relationships in Metal Complexes. Part 3.† The Electrochemical Activation of Co-ordinated Hydrazido(2−)-ligands

By **Brian A. L. Crichton, Jonathan R. Dilworth,** and **Christopher J. Pickett,*** A.R.C. Unit of Nitrogen Fixation, University of Sussex, Brighton BN1 9RQ
Joseph Chatt, School of Molecular Sciences, University of Sussex, Brighton BN1 9QJ

The complexes $[Mo(N_2RR')(S_2CNMe_2)_3]^+$, R,R′ = alkyl or aryl, undergo two successive reversible one-electron reductions in non-aqueous electrolytes at platinum or vitreous carbon electrodes. The initial electron-transfer product $[Mo(N_2RR')(S_2CNMe_2)_3]^0$ disproportionates to $[Mo(N_2RR')(S_2CNMe_2)_3]^+$ and to the product of the second electron transfer, $[Mo(N_2RR')(S_2CNMe_2)_3]^-$. Two-electron reduction of the cation leads to electroactivation of the N_2RR' ligand towards attack by electrophiles and reduction/protonation is shown to liberate the free hydrazine, $NH_2NMe(Ph)$, in *ca.* 57% yield. A plausible mechanism for this electroactivation is discussed, and, from studies of related complexes, it is suggested that the redox orbitals of the $[Mo(N_2R_2)(S_2CNMe_2)_3]^+$ complex are associated with the Mo=N–N function.

ELECTRON transfer to a moiety containing the $Mo=NNH_2$ group may be a step in the nitrogen-fixing process catalysed by nitrogenase.[1] The electrochemical reactions of complexes containing such groups, $Mo\overset{\leftarrow}{=}NNR_2$, R = H, alkyl, or aryl, are therefore of interest in this context as well as from a broader viewpoint, that of electroactivation of co-ordinated ligands and of relationships between structure, redox potential, and reactivity.

In previous papers we have discussed the electrochemical behaviour of certain complexes containing the $Mo\leftarrow N_2$ and Mo–N=NR functions (R = alkyl or aryl) in terms of the influence of the co-ordination environment of the Mo upon the redox potential of these complexes and how their electrochemical behaviour is related to certain other properties such as reactivity towards electrophiles and nucleophiles, vibrational and electronic spectra.[2-5] In this paper we consider the electrochemical properties of some dithiocarbamato-complexes of Mo containing the $Mo=NNR_2$ function. These complexes formally represent a further stage of reaction of a co-ordinated N_2 ligand with R^+, although in this instance the complexes are prepared from a hydrazine rather than co-ordinated N_2, equation (1).

$$Mo(N_2) \xrightarrow{R^+} Mo(N_2R)^+ \xrightarrow{R^+} Mo(N_2R_2)^{2+} \quad (1)$$

RESULTS AND DISCUSSION

Electrochemical Reduction of Complexes $[Mo(N_2RR')(S_2CNMe_2)_3]^+$, $(A)^+$.—*Structure of the complexes.* The complexes $[Mo(N_2RR')(S_2CNMe_2)_3]^+$, $(A)^+$, R,R′ = alkyl or aryl, have the Mo centre formally in the 6+ oxidation state and they are diamagnetic. The structure of the complex $[Mo(N_2RR')\{S_2CN(CH_2)_5\}_3]^+$, R = Et, R′ = Ph, has been determined by *X*-rays: the co-ordination geometry is essentially pentagonal bipyramidal with the N_2RR' group occupying an apical position.[6] The Mo–N bond is relatively short and the Mo–N–N group is essentially linear. This is consistent with the hydrazido(2−)-ligand functioning as a four-electron donor to the molybdenum atom and hence conferring on the complex an 18-e closed-shell configuration. Undoubtedly, this type of structure also pertains to the complexes $(A)^+$ investigated in this work.

Elementary electron-transfer reactions of the complexes $(A)^+$. Cyclic voltammetry of $(A)^+$ at platinum or vitreous carbon electrodes in 0.2 mol dm^{-3} $[NBu_4][BF_4]$–tetrahydrofuran (thf) or methyl cyanide show two one-electron reduction steps at moderately negative potentials. The first process is electrochemically reversible for each complex at scan rates >0.3 V s^{-1}, whilst the second electron transfer shows electrochemical reversibility only at scan rates >10 V s^{-1}. Figure 1 shows a typical cyclic voltammogram for the complexes $(A)^+$ and Table 1 lists the appropriate electrochemical data. The elementary electron-transfer reactions of $(A)^+$ may be summarised according to Scheme 1.

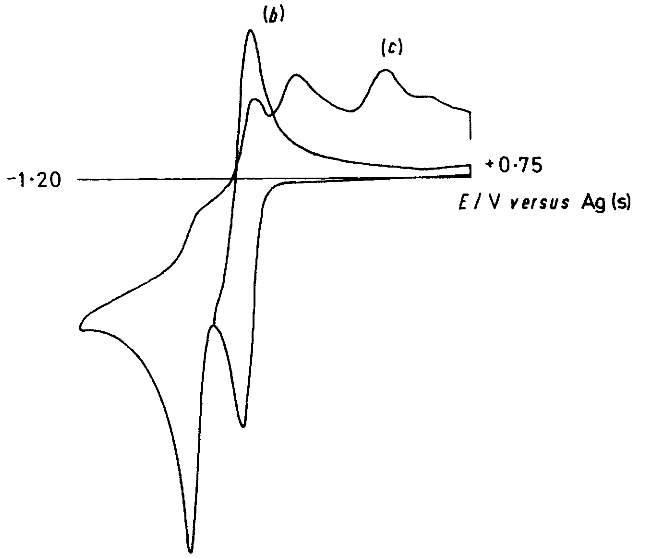

FIGURE 1 Cyclic voltammogram of *ca.* 5 mmol dm^{-3} $[Mo(NNMePh)(S_2CNMe_2)_3]^+$ in thf–0.2 mol dm^{-3} $[NBu_4][BF_4]$ at a platinum wire electrode. Scan rate 0.15 V s^{-1}. Ag(s)–electrolyte pseudo-reference electrode. The oxidation waves (*b*) and (*c*) correspond to the intermediate (B) and product (C) respectively, generated by the second reduction process

The complexes $[Mo^V(N_2RR')(S_2CNMe_2)_3]^0$, $(A)^0$. The neutral species, $(A)^0$, are not indefinitely stable in the

---

† Part 2 is ref. 3.

electrolyte media at ambient temperatures (*ca.* 20 ± 2 °C), their half-lives being in the order of several seconds. However, a stable solution of $(A)^0$ (R = Me, R′ = Ph) may be prepared by controlled-potential electrolysis of $(A)^+$ at 0 °C ($^{1}E_{\rm p}^{\rm red}$ + 100 mV) in thf–0.2 mol dm^{-3} $[NBu_4][BF_4]$. The current decays after the passage of 1 Faraday mol^{-1} to a background level whilst the solution changes in colour from the orange-brown of $(A)^+$ to purple. Examination of the catholyte by cyclic voltammetry after the 1 Faraday mol^{-1} reduction indicates the formation of $(A)^0$. Examination of a sample of the frozen catholyte solution at −145 °C by e.s.r. reveals a paramagnetic signal, which we attribute to $(A)^0$, characterised by $g_1 = 1.995\,9$, $g_2 = 1.968\,0$, and $g_3 = 1.957\,8$. The spectrum suggests that the unpaired electron density is located on the Mo centre: molybdenum hyperfine lines observed, $\langle A_{\rm Mo}\rangle = 6.2$ mT, are consistent with an interaction between ^{97}Mo and ^{95}Mo, spin $\frac{5}{2}$. The spectrum of the 19-e species suggests predominantly axial symmetry with some rhombic distortion ($g_2 \approx g_3$). This is consistent with retention of the (presumed) pentagonal-bipyramidal geometry of its 18-e precursor, $(A)^+$. In this respect the spectrum is similar to that of the 17-e molybdenum(V) species $[Mo(N_2Ph)(S_2CNMe_2)_3]^+$ which also retains the axial symmetry of its 18-e pentagonal-bipyramidal parent.[2]

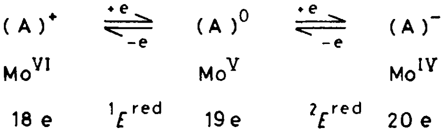

SCHEME 1

The mechanism of the decomposition of $(A)^0$. The cyclic voltammogram of the complexes $(A)^+$ at ambient temperatures reveals that the one-electron reduction products $(A)^0$ are somewhat unstable and undergo a reaction followed by electron transfer. Thus the peak current ratio, $^{1}i^{\rm ox}_{\rm p}/^{1}i_{\rm p}^{\rm red}$, deviates from unity at the slower scan rates, ν, whilst the peak current function $^{1}i_{\rm p}^{\rm red}\,.\,\nu^{-\frac{1}{2}}$ approaches that for an overall two-electron reduction, Figure 2.

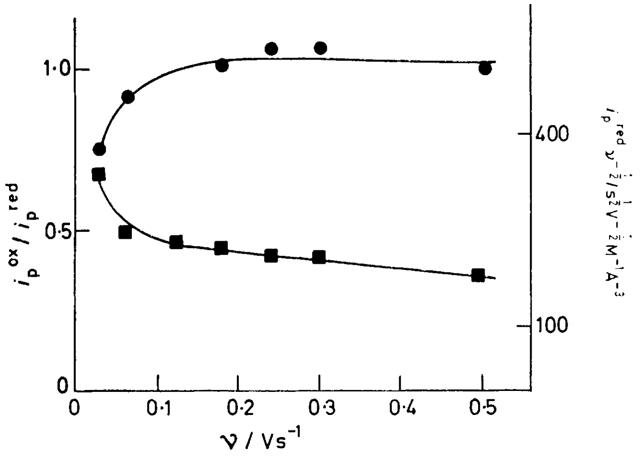

FIGURE 2 The stability of the complex $[Mo(NNMePh)(S_2CNMe_2)_3]^0$. Peak current ratio ($i_{\rm p}^{\rm ox}/i_{\rm p}^{\rm red}$) (●) and peak current function ($^{1}i_{\rm p}^{\rm red}/\nu^{\frac{1}{2}}$) (■) *versus* the scan rate, ν, from cyclic voltammetry of $(A)^+$ (2.1 mmol dm^{-3}) in 0.2 mol dm^{-3} $[NBu_4][BF_4]$–acetonitrile at a platinum wire electrode

The intermediates produced upon cyclic voltammetry into the second reduction process, (B) and (C), which are characterised by the oxidation waves (*b*) and (*c*) respectively, Figure 1, also appear after holding the potential at $^{1}E_{\rm p}$ + 100 mV for *ca.* 60 s prior to scan reversal.

Controlled-potential electrolysis at a potential of $^{1}E_{\rm p}$ + 100 mV at *ca.* 20 °C tends towards a two-electron overall reduction whilst the current against charge passed plots are non-linear at this potential, consistent with the cyclic voltammetry, Figure 3. Controlled-potential reduction at potentials $^{2}E_{\rm p}$ + 100 mV show linear current against charge passed plots with the consumption of 2 F per mol of complex, Figure 4. Examination of the catholytes by cyclic voltammetry after *either* the $^{1}E_{\rm p}$ + 100 mV *or* the $^{2}E_{\rm p}$ + 100 mV two-electron reductions show that a single major product, (C), characterised by the oxidation process (*c*), Figure 1, has been formed.

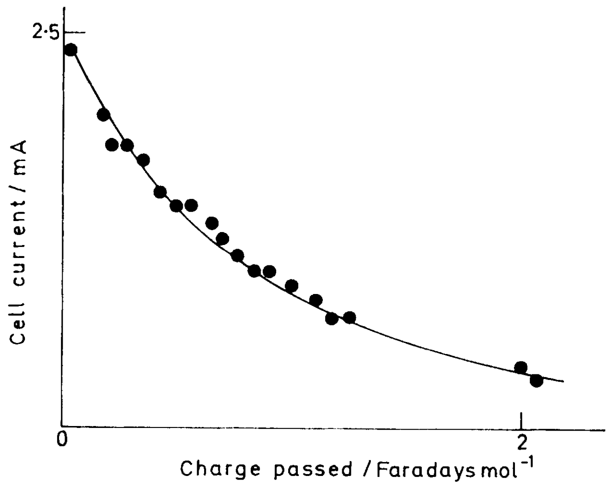

FIGURE 3 Plot of charge passed *versus* cell current for the electrolysis of $[Mo(NNMePh)(S_2CNMe_2)_3]Br$ in thf–0.2 mol dm^{-3} $[NBu_4][BF_4]$ at a platinum gauze electrode. Electrolysis was carried out at −0.74 V *versus* s.c.e. on 23.1 mg of sample in 20 cm^3 of catholyte under N_2

These results are entirely consistent with a disproportionation mechanism with the regeneration of electroactive $(A)^+$ and unstable $(A)^-$ [equation (2)].

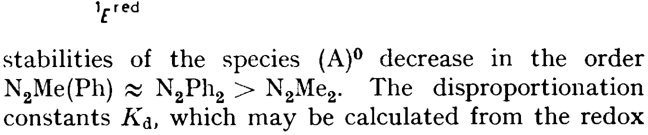

The stabilities of the species $(A)^0$ decrease in the order $N_2Me(Ph) \approx N_2Ph_2 > N_2Me_2$. The disproportionation constants $K_{\rm d}$, which may be calculated from the redox potential data and which are listed in Table 1, decrease in the order $N_2Ph_2 > N_2Me(Ph) > N_2Me_2$. Evidently, k_1 must be larger with the more electron-donating N_2Me_2

TABLE 1

Electrochemical data for complexes $[Mo(N_2RR')(S_2CNMe_2)_3]^+$ determined by cyclic voltammetry *

Complex	${}^1E_{\frac{1}{2}}^{red}/V$	${}^1\|E_p^{red} - E_p^{ox}\|/mV$	(i_p^{ox}/i_p^{red})	${}^2E_p^{red}/V$	$\Delta E/mV$	${}^1n$	${}^2n_{app.}$	10^5K_d 298 K
$[Mo(NNMe_2)(S_2CNMe_2)_3]^+$	−0.77	80	1.1	−1.05	45	1 (0.9)	1 (0.9)	5
$[Mo(NNMePh)(S_2CNMe_2)_3]^+$	−0.61	60	1.1	−0.90	40	1 (1.0)	1 (1.0)	10
$[Mo(NNPh_2)(S_2CNMe)_3]^+$	−0.58	70	1.05	−0.85	40	1 (1.0)	1 (1.0)	5
$[Mo(NNMe_2)\{S_2CN(CH_2)_5\}_3]^+$	−0.77	100	1.1	−1.06	45	1 (0.9)	1 (0.9)	5
$[MoN(S_2CNMe_2)_3]$	−0.40	150				1 (0.8)		
Range	±0.01 V	±5 mV	±0.05	±0.01 V	±5 mV	±0.1	±0.1	±3

* In 0.2 mol dm^{-3} $[NBu_4][BF_4]$–acetonitrile at a platinum electrode. $\Delta E = {}^2E_p^{red} - {}^2E_{\frac{p}{2}}^{red}$. The values of ${}^1n$ and ${}^2n$ are the numbers of electrons involved in the primary and secondary electrode processes respectively.

group attached to the Mo. That $Me_2NN=$ is more donating is reflected by the *ca.* 190 mV difference between the reduction potential of the complex with this ligand and the complex with the $Ph_2N_2=$ ligand, Table 1.

The formation of free organohydrazine via *electrochemical activation of the* $Mo(N_2MePh)$ *group.* Two-electron reduction of $(A)^+$ (R = Me, R′ = Ph) gives the stable product (C) at potentials close to ${}^1E_p^{red}$ or ${}^2E_p$ in thf or MeCN electrolytes as discussed above. (C) reacts rapidly with HCl–diethyl ether as evidenced by the immediate discharge of the oxidation peak (*c*) observed upon cyclic voltammetry of (C). Base extraction and analysis by gas–liquid chromatography (g.l.c.) reveals that (C) has been converted to the free hydrazine $NH_2NMe(Ph)$ in *ca.* 57% yield: less than 1% amine was detected, equation (3).

$$(A)^+ \xrightarrow{+\ 2e} (C) \xrightarrow[\substack{\text{(ii) excess of} \\ \text{aqueous K[OH]} \\ (40\%) \\ \text{(iii) diethyl ether} \\ \text{extraction}}]{\text{(i) H}^+} \underset{ca.\ 57\%}{NH_2NMe(Ph)} \qquad (3)$$

Treatment of $(A)^+$ in thf with HCl–diethyl ether does not produce $NH_2NMe(Ph)$ and indeed no reaction is evident. Less than 1% of the free hydrazine is detected after 2-e reduction and examination of the catholyte by g.l.c. without the acidification and work-up steps. Clearly the electro-reduction activates the $MoN_2Me(Ph)$ group towards protic attack.

The mechanism of hydrazine formation: the nature of the intermediate (B) *and product* (C). We have not been able to isolate and characterise the reactive product (C). It clearly retains an organodinitrogen group bound to the Mo as the hydrazine $NH_2NMe(Ph)$ is not released until (C) is destroyed by acid. Nevertheless, certain conclusions as to the nature of the product (C) and its precursor (B) may be drawn from a consideration of the redox potential data in Tables 1 and 2.

First, the complexes $(A)^+$ do *not* give diazenido-complexes upon reduction (4). This reaction is eliminated as the R = Me or Ph complexes (D) oxidise at

$$[Mo(NNR_2)(S_2CNMe_2)_3]^+ \xrightarrow[H^+]{+\ 2e} \underset{(D)}{[Mo(NNR)(S_2CNMe_2)_3]} + RH \qquad (4)$$

considerably more positive potentials than (B) or (C) and it would be inconsistent with the formation of $NH_2NMe(Ph)$.

Secondly, the absence of significant amounts of the amine NHMe(Ph) as a product of the reaction of (C) with acid and the absence of an oxidation or reduction process assignable to the nitride $[MoN(S_2CNMe_2)_3]$ eliminates the reduction (5). Finally, the formation of $[Mo(S_2CNMe_2)_2$-

TABLE 2

Electrochemical data for complexes $[Mo(N_2RR')(S_2CNMe_2)_2X_2]$ and some related species determined by cyclic voltammetry [a]

	Primary reduction process				Primary oxidation process					
Complex	${}^1E_p^{red}/V$	Δ^1E^a/mV	$i_p\nu^{-\frac{1}{2}}c^{-1}/s^{\frac{1}{2}}V^{-\frac{1}{2}}M^{-1}A^{-3}$	$n_{app.}$ [b]	E_p^{ox}/V	E_p^{red}/V	$E_p^{ox} - E_p^{red}/mV$	E^a/mV	$i_p\nu^{-\frac{1}{2}}c^{-1}/s^{\frac{1}{2}}V^{-\frac{1}{2}}M^{-1}A^{-3}$	$n_{app.}$ [b]
(1) $[MoO(NNMe_2)(S_2CNMe_2)_2]$	−1.70	110	1.9	1 (0.8)	0.92			120	1.8	1 (0.7)
(2) $[MoO\{NN(Me)Ph\}$-$(S_2CNMe_2)_2]$	−1.54	94	1.7	1 (0.7)	1.06			97	1.7	1 (0.7)
(3) $[MoO(NNPh_2)(S_2CNMe_2)_2]$	−1.50	115	1.7	1 (0.7)	1.13			118	1.7	1(0.7)
(4) $[MoO\{NN(Me)Ph\}_2$-$(S_2CNMe_2)_2]$	−2.50	120	2.4	1	0.42	+0.38	40	55	2.6	1 (1.0)
(5) $[MoCl_2(NNMe_2)$-$(S_2CNEt_2)_2]$	−1.18	128	2.7	1 (1.1)	1.30	+1.23	70	60	2.5	1 (1.0)
(6) $[MoCl_2\{NN(Me)Ph\}$-$(S_2CNMe_2)_2]$	−0.99	144	2.2	1 (0.9)	1.37	+1.32	50	61	1.8	1 (0.7)
(7) $[MoCl_2(NNPh_2)$-$(S_2CNMe_2)_2]$	−0.87	130	2.6	1 (1.0)	1.41	+1.36	50	55	2.0	1 (0.8)
(8) $[MoN(S_2CNEt_2)_3]$	−0.40	150	1.8	1 (0.8)	1.39			154	1.2	1 (0.5)
(9) $[MoO_2(S_2CNEt_2)_2]$	−0.85	80	2.0	1 (0.7)	No oxidation process					
(10) $[MoOCl_2(S_2CNEt_2)_2]$	−0.32	114	2.1	1 (0.7)	No oxidation process					
Range	±0.01 V	±5 mV	±0.1	±0.1	±0.01 V	±0.01 V	±5 mV	±5 mV	±0.1	±0.1

[a] In 0.2 mol dm^{-3} $[NBu_4][BF_4]$–acetonitrile at a platinum electrode, scan rate 0.3 V s^{-1}. M = mol dm^{-3}. [b] Values of $n_{app.}$, the apparent number of electrons involved in the irreversible electron-transfer steps, were determined by comparison of their current functions at 0.3 V s^{-1} with that for ferrocene oxidation at the same electrode, for which $i_p\nu^{-\frac{1}{2}}[\text{ferrocene}]^{-1} = 2.5\ s^{\frac{1}{2}}V^{-\frac{1}{2}}M^{-1}A^{-3}$.

$(N_2R_2)_2]$ or $[MoO(S_2CNMe_2)_2(N_2R_2)]$ complexes, which might be conceivably found *via* partial decomposition

$$[Mo(N_2R_2)(S_2CNMe_2)_3]^+ \xrightarrow[H^+]{+2e} [MoN(S_2CNMe_2)_3] + NHR_2 \quad (5)$$

of the co-ordination shell of Mo upon reduction, were not detected electrochemically during cyclic voltammetry or controlled-potential electrolyses of $(A)^+$.

The addition of two electrons to the 18-e $(A)^+$ to give the 20-e species $(A)^-$ must result in considerable electronic strain. This may be relieved by decomposition of $(A)^-$ either by ligand dissociation (6) or by rearrangement of the electrons in the hydrazido(2−)-ligand (7). Reorganisation of ligands around a metal centre, *e.g. cis*-to-*trans* isomerism, can induce changes in oxidation potential of the order of 500 mV or less. The difference in oxidation potentials of the initial reduction product $(A)^-$ and that of the intermediate (B) is *ca.* 300 mV; this stabilisation of the redox orbital upon conversion of $(A)^-$ to (B) would be consistent with the rearrangement (6) or (7).

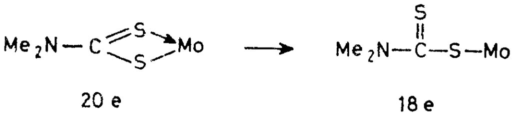

(6)

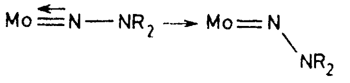

(7)

The oxidation potential of the product (C) differs from that of $(A)^0$ by some 700 mV and from that of $(A)^-$ by some 1 000 mV. This is consistent with charge neutralisation upon the conversion $(A)^- \longrightarrow (C)$. For example, the oxidation potentials of $[Mo(N_2Ph)(S_2CNMe_2)_3]$ and $[Mo(N_2PhMe)(S_2CNMe_2)_3]^+$ differ by *ca.* 1 100 mV. Charge neutralisation could take place by either protonation of (B) or *via* loss of an anionic ligand from it. We did not detect oxidation waves attributable to free $S_2CNMe_2^-$ and therefore suggest that stabilisation is a consequence of protonation on the α-N atom, reaction (8). Complexes of Mo containing the side-on $NHNR_2$ group have recently been characterised by *X*-ray analysis, moreover, further protonation of these yield hydrazines.[7]

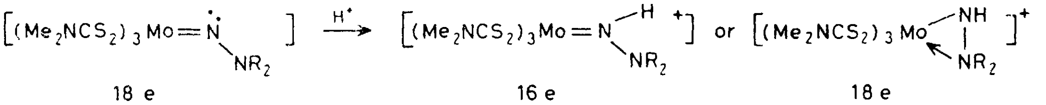

(8)

Support for an electrophilic attack upon the species $(A)^-$ or (B) is as follows. Cyclic voltammetry of $(A)^+$ (R = Me, R′ = Ph) in the presence of a ten-fold excess of MeI results in the loss of the product oxidation waves (*b*) and (*c*), Figure 1, whilst a new peak which corresponds to the oxidation of free iodide ion is observed. The compound Pr^nBr has a similar effect although considerably less marked. Controlled-potential electrolysis of $(A)^+$ in the presence of an excess of MeI *remains* an overall 2-e reduction: this excludes the oxidative regeneration of $(A)^0$ as a possible reaction as this must consume >2 e per molecule of complex. The product (C) which rapidly reacts with HCl is also sufficiently nucleophilic to react with one equivalent of MeI.

The identity of the metal product following protonation of (C) remains elusive. A broad reduction wave observed after the addition of HCl–diethyl ether to a thf catholyte containing (C) may possibly be associated with the reduction of $[MoCl(S_2CNMe_2)_3]$ although this is by no means certain.

In conclusion, we have shown that the MoNNRR′ group in $(A)^+$ is activated towards protonation by electroreduction, but have not been able to establish unambiguously the mechanism of the activation. A plausible reaction sequence based on the above data is advanced in Scheme 2.

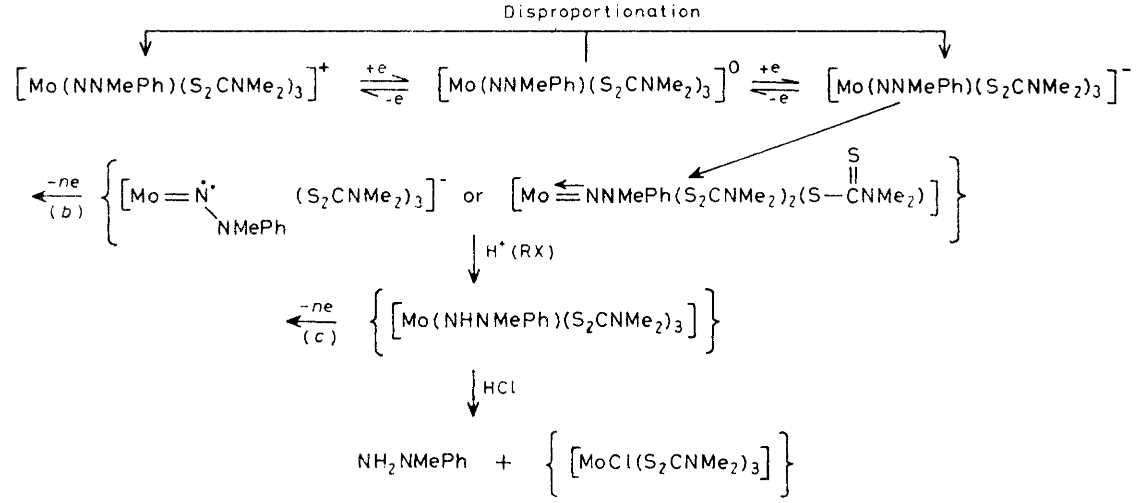

SCHEME 2 Electroactivation of Mo=NNMePh towards protic attack. Species in braces are non-isolated intermediates; (*b*) and (*c*) refer to the oxidation waves of Figure 1

Influence of the Ligand Environment of Mo=NNR$_2$ *Complexes upon their Redox Behaviour.*—The effect of changing R or R′ in the complexes (A)$^+$ upon their reduction potential is minimal: the expected trend is observed, with $^1E_{\frac{1}{2}}{}^{\mathrm{red}}$ more positive in the order N$_2$Me$_2$ < N$_2$Me(Ph) < N$_2$Ph$_2$ (Table 1).

Reduction and oxidation potential data for some related complexes [Mo(N$_2$RR′)(S$_2$CNMe$_2$)$_2$X$_2$] in which X = $\frac{1}{2}$O, Cl, or $\frac{1}{2}$NNRR′ are listed in Table 2. The influence of a change in R or R′ upon the reduction and oxidation potentials of these complexes follows the same trend as in the complexes (A)$^+$. What is more interesting is the influence of X. Each complex reduces in an irreversible one-electron step at scan rates up to 10 V s^{-1} and oxidises more or less irreversibly in a one-electron process. The influence of X is substantial: oxidation *and* reduction potentials, $^1E_p{}^{\mathrm{ox}}$ and $^1E_p{}^{\mathrm{red}}$ respectively, become increasingly positive in the order of X, $\frac{1}{2}$N$_2$RR′ < $\frac{1}{2}$O < Cl. There is an excellent correlation between $^1E_p{}^{\mathrm{ox}}$ and $^1E_p{}^{\mathrm{red}}$ for the two redox processes and the slope of Figure 5 demonstrates that the lowest unoccupied molecular orbital, l.u.m.o., responds to a change in X to much the same extent as does the highest occupied molecular orbital, h.o.m.o. Some caution is necessary in the interpretation of the redox data as $^1E_p{}^{\mathrm{ox}}$ and $^1E_p{}^{\mathrm{red}}$ are not purely thermodynamic. Nevertheless, the implications are that the l.u.m.o. has substantial metal character. The complex (A)$^+$; R = Me, R′ = Ph lies upon the redox potential plot, Figure 4, whereas the complexes [MoO$_2$(S$_2$CNMe$_2$)$_2$] and [Mo(≡N)(S$_2$CNMe$_2$)$_3$] do not, and we may conclude that the h.o.m.o. and the l.u.m.o. are therefore both associated with the Mo=N–NR$_2$ system.

Conclusions.—It has been suggested that the reduction of an intermediate containing the linear Mo=NNH$_2$ group may be a step in the catalytic reduction of dinitrogen *via* nitrogenase.[5] We have demonstrated that 2-e reduction of certain 18-e complexes containing the Mo=NNR$_2$ group can lead to the activation of the organodinitrogen ligand towards attack by electrophiles, and in one case that reduction/protonation leads to the liberation of free organohydrazine in *ca.* 57% yield.

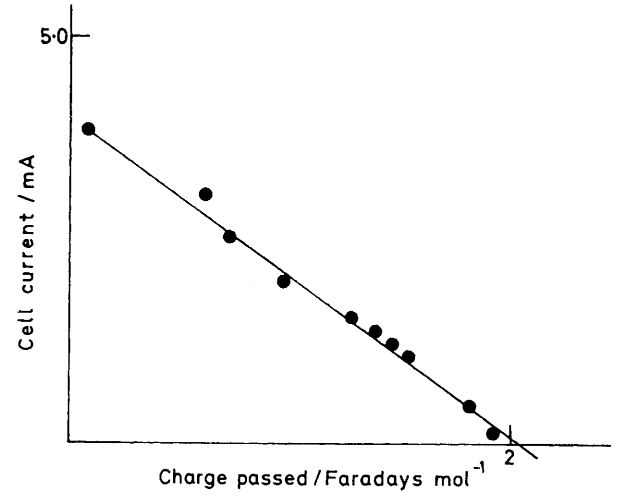

FIGURE 4 Plot of charge passed *versus* cell current for electrolysis of [Mo(NNMePh)(S$_2$CNMe$_2$)$_3$]Br in thf–0.2 mol dm^{-3} [NBu$_4$][BF$_4$] at a platinum gauze electrode. Electrolysis was carried out at −1.0 V *versus* s.c.e. on 26.9 mg of sample in 20 cm^3 of catholyte under N$_2$

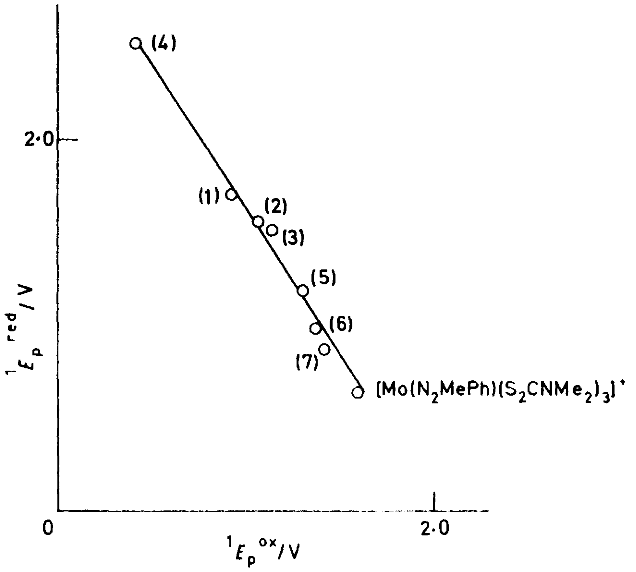

FIGURE 5 Correlation of reduction and oxidation potentials. Plot of $^1E_p{}^{\mathrm{red}}$ *versus* $^1E_p{}^{\mathrm{ox}}$ for various dithiocarbamato-complexes of Mo$^{\mathrm{VI}}$ containing the MoNNRR′ group. Slope of d($^1E_p{}^{\mathrm{red}}$)/d($^1E_p{}^{\mathrm{ox}}$) = 1.63 (dimensionless). The numbering corresponds to that of the complexes in Table 2

EXPERIMENTAL

The preparations of the complexes investigated have been described elsewhere.[8,9] The solvents and the electrolyte were purified and dried by standard procedures.

Cyclic voltammetry was carried out in oxygen-free electrolytes under an atmosphere of dinitrogen using a two-compartment, three-electrode electrochemical cell, a Hi-Tek Instruments Ltd. DT2101 potentiostat, and a Chemical Electronics (Birtley) Ltd. type 01 waveform generator. Voltammograms were recorded on a Philips PM8041 *X–Y* recorder at ambient temperature, 20 ± 2 °C.

Controlled-potential electrolyses were performed in an H-type three-electrode, three-compartment cell with a working electrolyte volume of 20 cm^3. Platinum gauze working and auxiliary electrodes of nominally 1 cm^2 were employed. Electrolyses were carried out on 50—100 µmol of complex under a dinitrogen atmosphere and the charge passed was measured using a Chemical Electronics integrator.

After electrolysis the catholyte was quenched with an excess of HCl–diethyl ether and removed from the cell. An equal volume, *ca.* 20 cm^3, of 40% aqueous K[OH] was added to the catholyte and the resulting solution extracted three times with diethyl ether in 20-cm^3 aliquots. The ether extracts were combined and reduced in volume to 20 cm^3 and examined by g.l.c. on a Carbopak 4% Carbowax (20 mol dm^{-3})–0.8% K[OH] column at 150 °C. Under these conditions NHMePh had a retention time of *ca.* 3 min and NH$_2$NMePh a retention time of *ca.* 6 min. Acetonitrile electrolyses gave substantially lower yields of the hydrazine (5—7%) than did the thf electrolysis of the complex [Mo(N$_2$MePh)(S$_2$CNMe$_2$)$_3$]$^+$. This may be attributed to the condensation of the hydrazine with hydrolysis products of CH_3CN.

Electron spin resonance spectra were recorded on a Varian Associates Ltd. E9 spectrometer.

We thank Miss J. E. Kendrick for experimental assistance.

[0/1070 *Received, 7th July*, 1980]

REFERENCES

[1] G. J. Leigh and C. J. Pickett, *J. Chem. Soc., Dalton Trans.*, 1977, 1797.

[2] G. Butler, J. Chatt, G. J. Leigh, and C. J. Pickett, *J. Chem. Soc., Dalton Trans.*, 1979, 113.

[3] J. Chatt, G. J. Leigh, H. Neukomm, C. J. Pickett, and D. R. Stanley, *J. Chem. Soc., Dalton Trans.*, 1980, 121.

[4] J. Chatt, C. T. Kan, G. J. Leigh, C. J. Pickett, and D. R. Stanley, *J. Chem. Soc., Dalton Trans.*, 1980, 2032.

[5] R. N. F. Thorneley, J. Chatt, R. R. Eady, D. J. Lowe, M. J. O'Donnell, J. R. Postgate, R. L. Richards, and B. E. Smith in 'Nitrogen Fixation,' eds. W. E. Newton and W. H. Orme-Johnston, University Park Press, Baltimore, 1980, vol. 1, pp. 171—193.

[6] F. C. March, R. Mason, and K. M. Thomas, *J. Organomet. Chem.*, 1975, **96**, C43.

[7] J. A. Carroll, D. Sutton, M. Cowie, and M. D. Gauthier, *J. Chem. Soc., Chem. Commun.*, 1979, 1058; J. Chatt, P. L. Dahlstrom, J. R. Dilworth, and J. Zubieta, *ibid.*, 1980, 786.

[8] M. W. Bishop, J. Chatt, and J. R. Dilworth, *J. Organomet. Chem.*, 1974, **73**, C59.

[9] J. Chatt, B. A. L. Crichton, and J. R. Dilworth, unpublished work.